

MODIFIED CRLB ON THE MODULATION PARAMETERS OF A PSK SIGNAL

K. C. Ho

Department of Electrical Engineering, University of Missouri-Columbia, Columbia, MO 65211, USA.
Email: hod@missouri.edu

ABSTRACT

PSK is a common modulation format in digital communications. The estimation of modulation parameters is necessary for emitter interception in support of numerous military applications. This paper develops the Cramer-Rao Lower Bound for the modulation parameters of a PSK signal. The modulation parameters considered are the carrier frequency, the symbol time and the signal amplitude. The results show that the CRLB's for the modulation parameters are the same for M-ary PSK signals when $M > 2$. The CRLB's between BPSK and M-ary PSK with $M > 2$ are very close, although they are not exactly identical. The effect of pulse shaping on the CRLB of modulation parameters are also investigated.

1. INTRODUCTION

Many military applications are interested in intercepting a signal from an emitter, and analyzing the signal in support of intelligence, surveillance and target acquisition purposes. Quite often, a signal interceptor identifies the modulation format of an intercepted signal, and performs demodulation subsequently. Numerous methods have been proposed to identify the modulation type of a signal [1]-[4]. When the signal-to-noise ratio (SNR) is low, the knowledge of modulation parameters such as carrier frequency, symbol time are needed in order to achieve good identification accuracy. Demodulation of the signal also requires the modulation parameter values. In practice the modulation parameters of an intercepted signal are not known to a signal interceptor. Estimation of the parameters is therefore indispensable for emitter interception.

A popular digital modulation format is phase shift keying (PSK). This modulation scheme encodes digital data as phase changes in a carrier for the purpose of transmission. It is widely used nowadays especially in wireless communications, such as in the North America TDMA cellular standard IS-54 and the CDMA cellular standard IS-95.

This paper presents the Modified Cramer-Rao Lower Bound (MCRLB) [5] on the modulation parameters of a PSK signal. The modulation parameters considered in this

study are the carrier frequency, the symbol time and the signal amplitude. These parameters are different from those investigated in [5]. The PSK signal to be examined is general. It can have any modulation level and any pulse shaping waveform. The work in this paper will provide the upper bound on the estimation accuracy of modulation parameters, and will establish a baseline performance for any parameter estimation technique to compare against.

To demonstrate the usefulness of the results, we shall examine how the signaling level and different kinds of pulse shaping affect the CRLB. The paper is organized as follows. The following section describes the signal model from which the CRLB will be derived. Some common pulse shaping filters will also be summarized. The development of the CRLB is in Section 3. Section 4 presents simulation results on the parameter estimation accuracy at different signaling levels. It also examines the effects of pulse shaping on the CRLB. Finally, Section 5 concludes the paper.

2. SIGNAL MODEL

An M-ary PSK signal $s(t)$ has the form

$$s(t) = \alpha_I(t) \cos(2\pi f_c t) - \alpha_Q(t) \sin(2\pi f_c t), \quad (1)$$

where $\alpha_I(t)$ and $\alpha_Q(t)$ are the in-phase and quadrature component given by

$$\alpha_I(t) = \sum_n A \cos \phi_n g(t - nT_s), \quad (2)$$

$$\alpha_Q(t) = \sum_n A \sin \phi_n g(t - nT_s), \quad (3)$$

and

$$f_c = \text{carrier frequency,}$$

$$T_s = \text{symbol time,}$$

$$A = \text{signal amplitude,}$$

$$\phi_n \in \{ 2\pi m/M, m = 0, 1, \dots, M-1 \},$$

$$g(t) = \text{pulse shaping function.}$$

We assume here the carrier phase is zero to simplify the study. The purpose of pulse shaping is to improve the spec-

tral efficiency of a PSK signal. Some common pulse shaping functions are described below.

1. Raised Cosine (RC) Filter

The frequency response of a RC filter is

$$H_{RC}(f) = \begin{cases} 1 & 0 < |f| < \frac{1-\alpha}{2T_s} \\ \cos^2 \left[\frac{\pi T_s}{2\alpha} \left(f - \frac{1-\alpha}{2T_s} \right) \right] & \frac{1-\alpha}{2T_s} \leq |f| < \frac{1+\alpha}{2T_s} \\ 0 & |f| \geq \frac{1+\alpha}{2T_s} \end{cases} \quad (4)$$

and its impulse response is

$$h_{RC}(t) = \frac{\sin(\pi t/T_s) \cos(\pi \alpha t/T_s)}{(\pi t/T_s) (1 - 4\alpha^2 t^2/T_s^2)}, \quad (5)$$

where α is the roll-off factor between 0 and 1. The bandwidth of a RC filter is $(1 + \alpha)/2T_s$. The transmission is ISI free when a received signal is sampled at a period of T_s with correct timing.

2. Lowpass Filter

The frequency response and impulse response of an ideal lowpass filter are

$$H_{LP}(f) = \begin{cases} 1 & |f| < f_o \\ 0 & |f| \geq f_o \end{cases} \quad (6)$$

and

$$h_{LP}(t) = 2f_o \operatorname{sinc}(2f_o t). \quad (7)$$

The bandwidth of the lowpass filter is f_o .

3. CRLB OF A PSK SIGNAL

Let the intercepted signal be

$$x(t) = s(t) + n(t), \quad 0 < t \leq L \quad (8)$$

where $s(t)$ is a PSK signal, $n(t)$ is a white Gaussian noise of power σ^2 and L is the observation time. Define $\theta = [f_c, T_s, A]^T$ as the modulation parameter vector. Given the observation signal $x(t)$ for $0 < t \leq L$, we wish to find the CRLB of θ .

Since the noise $n(t)$ is Gaussian white, the probability density function (pdf) of $x(t)$ is

$$f(x(t), 0 < t \leq L; \theta) = K \exp \left\{ \frac{-1}{2\sigma^2} \int_0^L [x(t) - s(t; \theta)]^2 dt \right\} \quad (9)$$

where K is a constant and $s(t)$ is dependent on θ . The natural log of (9) is

$$\ln f(x(t), 0 < t \leq L; \theta) = \ln K - \frac{1}{2\sigma^2} \int_0^L [x(t) - s(t; \theta)]^2 dt. \quad (10)$$

The CRLB of θ is [?]

$$\text{CRLB} = \mathbf{J}^{-1} \quad (11)$$

where \mathbf{J} is the Fisher Information Matrix (FIM) defined as

$$\mathbf{J} = -E \left[\frac{\partial^2 \ln f}{\partial \theta \partial \theta^T} \right] \Bigg|_{\theta^\circ} \quad (12)$$

and θ° is the true parameter vector. Taking the derivative of (10) with respect to θ twice and evaluating it at θ° , we arrive at

$$\begin{aligned} \frac{\partial^2 \ln f}{\partial \theta \partial \theta^T} \Bigg|_{\theta^\circ} &= \frac{1}{\sigma^2} \int_0^L n(t) \frac{\partial^2 s(t; \theta^\circ)}{\partial \theta \partial \theta^T} \\ &\quad - \frac{1}{\sigma^2} \int_0^L \frac{\partial s(t; \theta^\circ)}{\partial \theta} \frac{\partial s(t; \theta^\circ)}{\partial \theta^T} dt. \end{aligned} \quad (13)$$

The expectation in (12) is taken over two random quantities. One is the random noise and the other is the digital data sequence (or the angle ϕ_n). Denote E_n as the expectation over noise and E_d as the expectation over the digital data sequence. Then

$$\begin{aligned} \mathbf{J} &= -E_d \left[E_n \left[\frac{\partial^2 \ln f}{\partial \theta \partial \theta^T} \Bigg|_{\theta^\circ} \right] \right] \\ &= \frac{1}{\sigma^2} \int_0^L E_d \left[\frac{\partial s(t; \theta^\circ)}{\partial \theta} \frac{\partial s(t; \theta^\circ)}{\partial \theta^T} \right] dt. \end{aligned} \quad (14)$$

From (1) the partial derivatives are

$$\frac{\partial s(t; \theta^\circ)}{\partial f_c} = -2\pi t [\alpha_I(t) \sin(2\pi f_c t) + \alpha_Q(t) \cos(2\pi f_c t)], \quad (15)$$

$$\frac{\partial s(t; \theta^\circ)}{\partial T_s} = \frac{\partial \alpha_I(t)}{\partial T_s} \cos(2\pi f_c t) - \frac{\partial \alpha_Q(t)}{\partial T_s} \sin(2\pi f_c t), \quad (16)$$

$$\frac{\partial s(t; \theta^\circ)}{\partial A} = \frac{1}{A} \alpha_I(t) \cos(2\pi f_c t) - \frac{1}{A} \alpha_Q(t) \sin(2\pi f_c t). \quad (17)$$

It can be shown that $\cos \phi_n$ and $\sin \phi_n$ are uncorrelated. Thus from (2) and (3)

$$\begin{aligned} E_d[\alpha_I(t) \alpha_Q(t)] &= E_d \left[\alpha_I(t) \frac{\partial \alpha_Q(t)}{\partial T_s} \right] \\ &= E_d \left[\frac{\partial \alpha_I(t)}{\partial T_s} \alpha_Q(t) \right] = E_d \left[\frac{\partial \alpha_I(t)}{\partial T_s} \frac{\partial \alpha_Q(t)}{\partial T_s} \right] \\ &= 0. \end{aligned} \quad (18)$$

As a result,

$$\begin{aligned} E_d \left[\left(\frac{\partial s(t)}{\partial f_c} \right)^2 \right] &= 4\pi^2 t^2 [E_d[\alpha_I^2(t)] \sin^2(2\pi f_c t) \\ &\quad + E_d[\alpha_Q^2(t)] \cos^2(2\pi f_c t)], \end{aligned} \quad (19)$$

$$E_d \left[\left(\frac{\partial s(t)}{\partial T_s} \right)^2 \right] = E_d \left[\left(\frac{\partial \alpha_I(t)}{\partial T_s} \right)^2 \right] \cos^2(2\pi f_c t) + E_d \left[\left(\frac{\partial \alpha_Q(t)}{\partial T_s} \right)^2 \right] \sin^2(2\pi f_c t), \quad (20)$$

$$E_d \left[\left(\frac{\partial s(t)}{\partial A} \right)^2 \right] = \frac{1}{A^2} [E_d[\alpha_I^2(t)] \cos^2(2\pi f_c t) + E_d[\alpha_Q^2(t)] \sin^2(2\pi f_c t)], \quad (21)$$

$$E_d \left[\frac{\partial s(t)}{\partial f_c} \frac{\partial s(t)}{\partial T_s} \right] = -\pi t \left\{ \left[E_d \left[\alpha_I(t) \frac{\partial \alpha_I(t)}{\partial T_s} \right] - E_d \left[\alpha_Q(t) \frac{\partial \alpha_Q(t)}{\partial T_s} \right] \right\} \sin(4\pi f_c t), \quad (22)$$

$$E_d \left[\frac{\partial s(t)}{\partial f_c} \frac{\partial s(t)}{\partial A} \right] = \frac{-\pi t}{A} \left\{ E_d[\alpha_I^2(t)] - E_d[\alpha_Q^2(t)] \right\} \sin(4\pi f_c t), \quad (23)$$

$$E_d \left[\frac{\partial s(t)}{\partial T_s} \frac{\partial s(t)}{\partial A} \right] = \frac{1}{A} \left\{ \left[E_d \left[\alpha_I(t) \frac{\partial \alpha_I(t)}{\partial T_s} \right] \cos^2(2\pi f_c t) + E_d \left[\alpha_Q(t) \frac{\partial \alpha_Q(t)}{\partial T_s} \right] \sin^2(2\pi f_c t) \right\}. \quad (24)$$

To proceed further, we shall consider BPSK and M-ary PSK ($M > 2$) separately.

3.1. BPSK

For BPSK, we have

$$\alpha_I(t) = A \sum_n a_n g(t - nT_s), \quad \alpha_Q(t) = 0 \quad (25)$$

where a_n is an IID sequence that takes on value 1 or -1 with equal probability. As a result,

$$E_d[\alpha_I^2(t)] = A^2 \sum_n g(t - nT_s)^2, \quad (26)$$

$$E_d \left[\alpha_I(t) \frac{\partial \alpha_I(t)}{\partial T_s} \right] = -A^2 \sum_n n g(t - nT_s) g'(t - nT_s), \quad (27)$$

$$E_d \left[\left(\frac{\partial \alpha_I(t)}{\partial T_s} \right)^2 \right] = A^2 \sum_n n^2 g'(t - nT_s)^2, \quad (28)$$

where $g'(t)$ is the derivative of $g(t)$ with respect to t . Consequently, putting (26)-(28) into (19)-(24), the elements of the FIM matrix in (14) are

$$J_{11} = \frac{4\pi^2 A^2}{\sigma^2} \int_0^L t^2 \sin^2(2\pi f_c t) \sum_n g(t - nT_s)^2 dt, \quad (29)$$

$$J_{22} = \frac{A^2}{\sigma^2} \int_0^L \cos^2(2\pi f_c t) \sum_n n^2 g'(t - nT_s)^2 dt, \quad (30)$$

$$J_{33} = \frac{1}{\sigma^2} \int_0^L \cos^2(2\pi f_c t) \sum_n g(t - nT_s)^2 dt, \quad (31)$$

$$J_{12} = J_{21} = \frac{\pi A^2}{\sigma^2} \int_0^L t \sin(4\pi f_c t) \sum_n n g(t - nT_s) g'(t - nT_s) dt, \quad (32)$$

$$J_{13} = J_{31} = \frac{-\pi A}{\sigma^2} \int_0^L t \sin(4\pi f_c t) \sum_n g(t - nT_s)^2 dt, \quad (33)$$

$$J_{23} = J_{32} = \frac{-A}{\sigma^2} \int_0^L \cos^2(2\pi f_c t) \sum_n n g(t - nT_s) g'(t - nT_s) dt. \quad (34)$$

Once the elements of the FIM \mathbf{J} are computed, taking the inverse of it yields the CRLB on θ .

3.2. M-ary PSK

In this case,

$$\alpha_I(t) = A \sum_n a_n g(t - nT_s), \quad a_n = \cos(2\pi m/M) \quad (35)$$

$$\alpha_Q(t) = A \sum_n b_n g(t - nT_s), \quad b_n = \sin(2\pi m/M) \quad (36)$$

where $0 \leq m \leq M - 1$ with equal probability of $1/M$. It can be easily verified that $E_d[a_n^2] = E_d[b_n^2] = 1/2$. Hence

$$E_d[\alpha_I^2(t)] = E_d[\alpha_Q^2(t)] = \frac{1}{2} A^2 \sum_n g(t - nT_s)^2, \quad (37)$$

$$E_d \left[\alpha_I(t) \frac{\partial \alpha_I(t)}{\partial T_s} \right] = E_d \left[\alpha_Q(t) \frac{\partial \alpha_Q(t)}{\partial T_s} \right] = \frac{-A^2}{2} \sum_n n g(t - nT_s) g'(t - nT_s), \quad (38)$$

$$\begin{aligned}
E_d \left[\left(\frac{\partial \alpha_I(t)}{\partial T_s} \right)^2 \right] &= E_d \left[\left(\frac{\partial \alpha_Q(t)}{\partial T_s} \right)^2 \right] \\
&= \frac{A^2}{2} \sum_n n^2 g'(t - nT_s)^2. \quad (39)
\end{aligned}$$

Substituting (37)-(39) to (19)-(24) and using (14) gives the elements of the FIM:

$$J_{11} = \frac{2\pi^2 A^2}{\sigma^2} \int_0^L t^2 \sum_n g(t - nT_s)^2 dt, \quad (40)$$

$$J_{22} = \frac{A^2}{2\sigma^2} \int_0^L \sum_n n^2 g'(t - nT_s)^2 dt, \quad (41)$$

$$J_{33} = \frac{1}{2\sigma^2} \int_0^L \sum_n g(t - nT_s)^2 dt. \quad (42)$$

$$J_{12} = J_{21} = J_{13} = J_{31} = 0, \quad (43)$$

$$J_{23} = J_{32} = \frac{-A}{2\sigma^2} \int_0^L \sum_n n g(t - nT_s) g'(t - nT_s) dt. \quad (44)$$

Now, applying (11) will give the CRLB of θ .

As seen in the derivation, M-ary PSK signals with $M = 2^l$ levels, $l > 1$, have the same CRLB. The CRLB for BPSK is different. However, the CRLB's for BPSK and M-ary PSK signals are very close, as will be demonstrated in the simulation section.

The FIM is dependent on g and g' . Hence the pulse shaping function affects the accuracy of parameter estimation. We shall examine through simulations on how the pulse shaping functions affect the parameter estimation accuracy.

4. SIMULATIONS

This section presents the numerical evaluation of the CRLB's for BPSK and M-ary PSK signals. The signal amplitude A was unity. The symbol time T_s was normalized to unity, f_c was set to $10/T_s$ and the observation time was 10 so that there were 10 symbols available for an estimator.

When the pulse shaping function was the RC filter as shown in (5), the CRLB's of f_c , T_s and A versus the roll-off factor α are depicted in Figures 1, 2 and 3 respectively. The modulation was BPSK. The CRLB values were normalized by the noise variance and were shown in the unit of dB. As the roll-off factor increases, the estimation accuracy for f_c decreases from -38.12dB to -37.00dB, T_s from -27.47dB

to -25.88dB and A from -6.9dB to -5.70dB. The CRLB of T_s seems to be saturated when the roll-off factor is larger than 0.8. We also evaluated the CRLB's for M-ary PSK modulation. The CRLB's from a M-ary PSK signal were slightly higher than that from a BPSK signal. The difference was, however, very small and insignificant.

If the pulse shaping function is the lowpass filter in (7), the CRLB's are shown in Figures 4-6. Only the results for BPSK are given because the results between BPSK and M-ary PSK were very close. When the bandwidth of the filter increases from $1/2T_s$ to $1/T_s$, the CRLB's of f_c and A are increased by about 3dB. However, the CRLB of T_s is decreased by 3dB.

5. CONCLUSIONS

We have derived the CRLB for the modulation parameters of a PSK signal. The modulation parameters considered are carrier frequency, symbol time and the signal amplitude. The CRLB is dependent on the observation time, the modulation parameters as well as the pulse shaping function. The CRLB was evaluated with the raised cosine and lowpass pulse shaping functions. The CRLB's of the three parameters increase when the roll-off factor in the RC filter increases. When the bandwidth of the lowpass filter is increased from $1/2T_s$ to $1/T_s$, the CRLB of f_c and A are increased by a factor of two. The CRLB of T_s , on the other hand, is decreased by a factor of two.

6. REFERENCES

- [1] S. Z. Hsue and S. S. Soliman, "Automatic modulation classification using zero crossing," *IEE Proceedings*, vol. 137, pp. 459-464, Dec. 1990.
- [2] A. Polydoros and K. Kim, "On the detection and classification of quadrature digital modulations in broadband noise," *IEEE Trans. Commun.*, vol. 38, pp. 1199-1211, Aug. 1990.
- [3] S. S. Soliman and S. Z. Hsue, "Signal classification using statistical moments," *IEEE Trans. Commun.*, vol. 40, pp. 908-916, May 1992.
- [4] C. Y. Huang and A. Polydoros, "Likelihood methods for MPSK modulation classification," *IEEE Trans. Commun.*, vol. 43, pp. 1493-1504, Feb/Mar/Apr. 1995.
- [5] F. Gini, R. Reggiannini and U. Mengali, "The modified Cramer-Rao bound in vector parameter estimation," *IEEE Trans. Commun.*, vol. 46, no. 1, pp. 52-60, Jan. 1998.

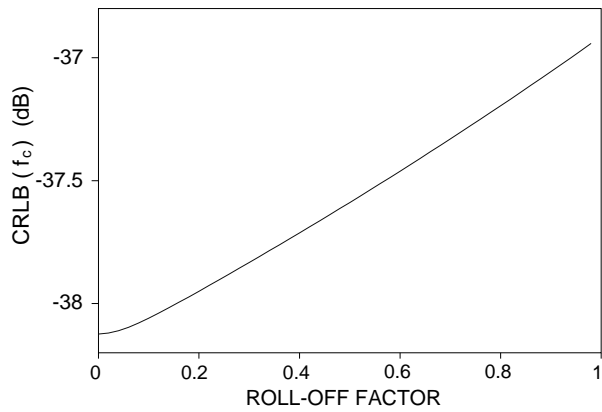


Figure 1: CRLB of f_c , RC pulse shaping function.

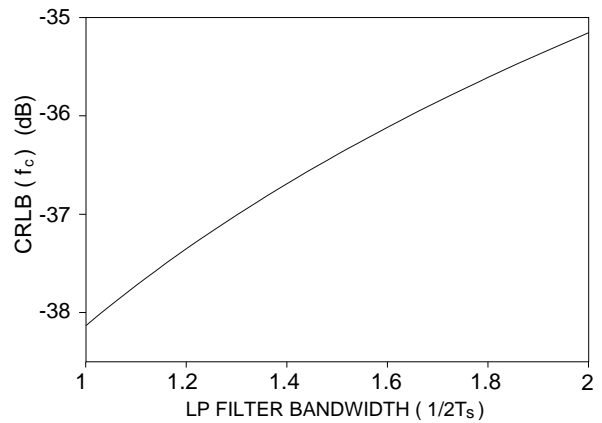


Figure 4: CRLB of f_c , lowpass pulse shaping function.

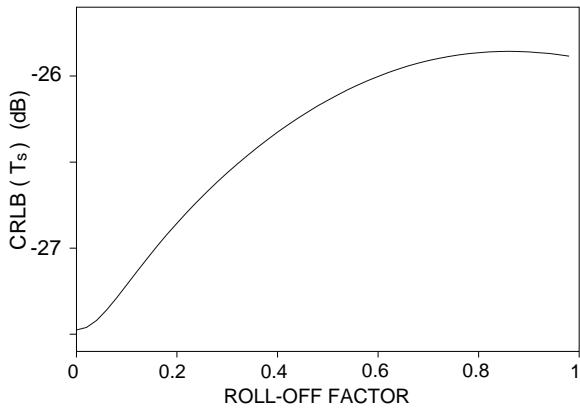


Figure 2: CRLB of T_s , RC pulse shaping function.

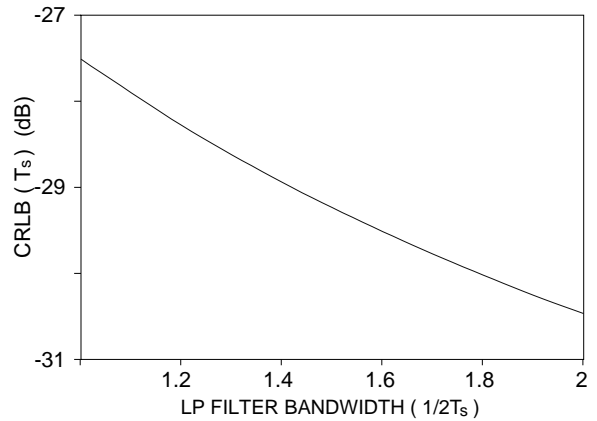


Figure 5: CRLB of T_s , lowpass pulse shaping function.

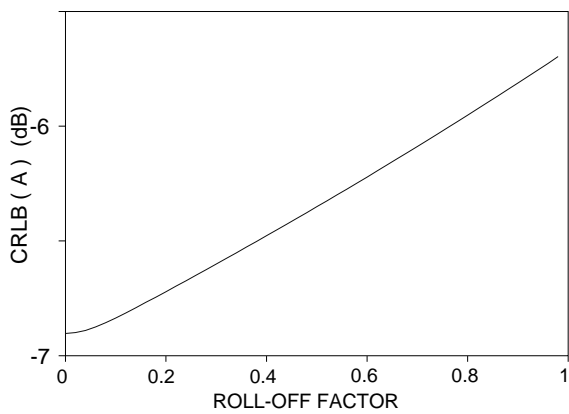


Figure 3: CRLB of A , RC pulse shaping function.

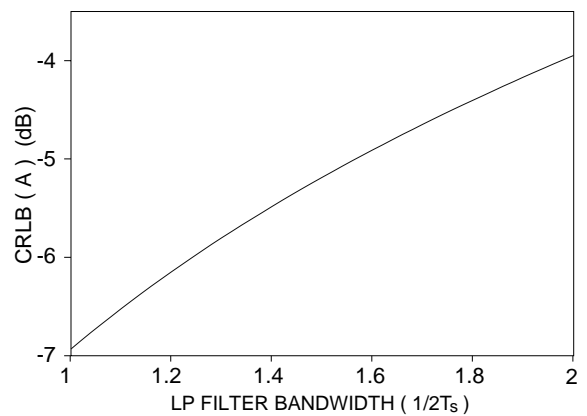


Figure 6: CRLB of A , lowpass pulse shaping function.